Original Article

Vascular

Vascular
2023, Vol. 31(4) 644–653

DOI: 10.1177/17085381221081324
journals.sagepub.com/home/vas
Sage

Mixed reality for the assessment of aortoiliac anatomy in patients with abdominal aortic aneurysm prior to open and endovascular repair: Feasibility and interobserver agreement

Johannes Hatzl, MD[1], Dittmar Böckler, MD[1], Niklas Hartmann[1], Katrin Meisenbacher, MD[1], Fabian Rengier, MD[2], Thomas Bruckner, PhD[3] and Christian Uhl, MD[1]

Abstract

Objectives: The objective is to evaluate the feasibility and interobserver agreement of a Mixed Reality Viewer (MRV) in the assessment of aortoiliac vascular anatomy of abdominal aortic aneurysm (AAA) patients.
Methods: Fifty preoperative computed tomography angiographies (CTAs) of AAA patients were included. CTAs were assessed in a mixed reality (MR) environment with respect to aortoiliac anatomy according to a standardized protocol by two experienced observers (Mixed Reality Viewer, MRV, Brainlab AG, Germany). Additionally, all CTAs were independently assessed applying the same protocol by the same observers using a conventional DICOM viewer on a two-dimensional screen with multi-planar reconstructions (Conventional viewer, CV, GE Centricity PACS RA1000 Workstation, GE, United States). The protocol included four sets of items: calcification, dilatation, patency, and tortuosity as well as the number of lumbar and renal arteries. Interobserver agreement (IA, Cohen's Kappa, κ) was calculated for every item set.
Results: All CTAs could successfully be displayed in the MRV (100%). The MRV demonstrated equal or better IA in the assessment of anterior and posterior calcification (κ_{MRV}: 0.68 and 0.61, κ_{CV}: 0.33 and 0.45, respectively) as well as tortuosity (κ_{MRV}: 0.60, κ_{CV}: 0.48) and dilatation (κ_{MRV}: 0.68, κ_{CV}: 0.67). The CV demonstrated better IA in the assessment of patency (κ_{MRV}: 0.74, κ_{CV}: 0.93). The CV also identified significantly more lumbar arteries (CV: 379, MRV: 239, $p < 0.01$).
Conclusions: The MRV is a feasible imaging viewing technology in clinical routine. Future efforts should aim at improving hologram quality and enabling accurate registration of the hologram with the physical patient.

Keywords

Mixed reality, augmented reality, virtual reality, EVAR, abdominal aortic aneurysm, Aneurysm

Introduction

In recent years, mixed reality (MR) technology has sparked great interest in the medical field. MR allows the projection of and interaction with holograms into the user's field of view by utilizing a head-mounted display (HMD).[1] By mixing a computer-generated virtual reality with the physical environment, many potential benefits seem accessible in a wide range of medical applications. This is inherently different from virtual reality, which is purely a simulated experience in which the use of computer modeling and simulation enables a person to

[1]Department of Vascular and Endovascular Surgery, University Hospital Heidelberg, Heidelberg, Germany
[2]Clinic for Diagnostic and Interventional Radiology, University Hospital Heidelberg, Heidelberg, Germany
[3]Institute of Medical Biometry and Informatics (IMBI), Heidelberg University, Heidelberg, Germany

Corresponding author:
Johannes Hatzl, Department of Vascular and Endovascular Surgery Heidelberg University Hospital Im Neuenheimer Feld 420, D-69120 Heidelberg 69120, Germany.
Email: johannes.hatzl@web.de

interact with a completely artificial three-dimensional environment.

MR can be applied to display a three-dimensional reconstruction of a patient's vascular anatomy derived from conventional computed tomography angiography (CTA). The three-dimensional holographic viewing experience of vascular disease potentially allows an improved understanding of complex vascular pathologies and might enable a new way of communicating that information to colleagues, patients, and students alike.

Among other areas, abdominal aortic aneurysms (AAAs) appear to be a promising field in which MR could prove to be a reasonable addon to existing technology. Technical and clinical success of endovascular aneurysm repair (EVAR) relies heavily on correct morphological assessment of the aortoiliac vasculature. By improving the three-dimensional understanding of diverse anatomical morphologies, MR could potentially prove to be a useful tool in preoperative planning and also intraoperative navigation during endovascular surgery.[2, 3] To date, some studies have been published aiming at the registration of three-dimensional holograms with the physical patient using semi-automatic and manual registration methods.[2, 4] The registration of the hologram with the real patient is the ultimate objective of MR applications in surgery but is currently limited to experimental single case studies with a focus on registration accuracy.[2, 4] However, to facilitate wide-spread adoption of this new technology in the future, one equally important prerequisites is a MR viewer application that allows production of high-quality holograms based on routine clinical data. This study presents such a tool and examines the feasibility and reliability of 50 produced holograms based on preoperative CTAs of AAA patients. Reliability is defined as the overall consistency of a measurement. One important component of reliability is the agreement of different observers when applying the same tool.[5] To date, the interobserver agreement (IA) of the assessment of aortoiliac anatomy displayed in a MR application is unknown. The aim of this validation study was to analyze IA for the assessment of aortoiliac anatomy in AAA patients in a MR environment and comparing it to the IA of a conventional viewer on a two-dimensional monitor.

Methods

Study design

This is a single center validation study examining the interobserver agreement (IA) of the assessment of aortoiliac anatomy of AAA patients in a three-dimensional MR environment compared to a conventional viewer on a two-dimensional monitor. Fifty preoperative CTAs of AAA patients were assessed in a MR environment according to a standardized protocol by two experienced observers (Mixed Reality Viewer, MRV, Brainlab AG, Munich, Germany). Both observers had at least 5 years of experience in the assessment of aortoiliac anatomy on conventional computed tomography angiography. There was no specific training required to assess aortoiliac anatomy in the MR environment. Additionally, all CTAs were independently assessed applying the same protocol by the same observers using a conventional DICOM viewer on a two-dimensional screen with axial, coronar, and sagittal reconstructions (Conventional viewer, CV, GE Centricity PACS RA1000 Workstation, Boston, Massachusetts, United States). Observers were blinded for the corresponding observer's assessment. The assessment of CTAs in either viewer was performed in random order and with a timely difference of at least 3 days between assessments in different viewers to prevent bias. Imaging pre-processing was performed by a third independent person. The protocol consisted of four sets of items including anterior and posterior calcification, dilatation, patency, and tortuosity as well as the number of lumbar and renal arteries. The primary endpoint was interobserver agreement in the assessment of calcification, dilatation, patency, and tortuosity (IA, (Cohen's kappa, κ). IA was calculated for every set and compared between viewers. Ethical approval was obtained by the local ethics committee (S-727/2020).

Mixed Reality Viewer

A dedicated MR workstation consisting of a personal computer (PC) running the Elements Viewer software (Brainlab AG, Munich, Germany), a Wi-Fi router, and an HMD was set up at the department of vascular and endovascular surgery.

The Elements Viewer software allows the automatic reconstruction of a three-dimensional model of the luminal vascular anatomy based on a CTA DICOM dataset applying the isosurface-volume-rendering method. The parietal thrombus volume is not automatically recognized by the software and must be added during post-processing. To assist in thrombus volume definition, the Elements SmartBruch (Brainlab AG, Munich, Germany) tool was utilized. This tool allows computer-assisted multi-planar outlining of thrombus volume and thereby creates a three-dimensional object that can be blended in with the remaining vascular reconstruction. Using the Elements SmartBruch, manual thrombus addition takes about 5–10 min depending on thrombus configuration and imaging quality. The three-dimensional reconstruction can then be projected in the user's field of view in a spatial computed environment via the HMD by scanning an automatically generated QR code that is being displayed on the monitor of the Elements Viewer software. The Magic Leap One (Magic Leap, Florida, USA) was used as an HMD in this study. The Magic Leap One is a head-mounted virtual

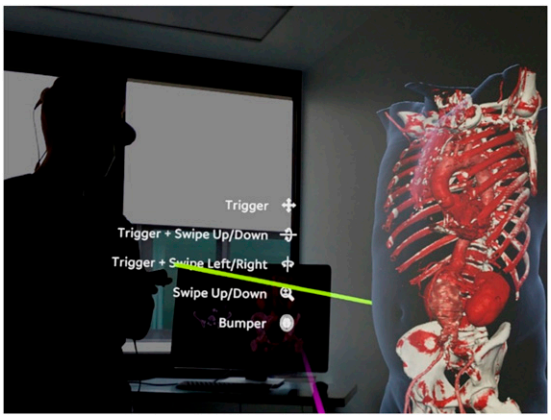

Figure 1. User's point of view examining aortoiliac anatomy of a AAA patient in the MR environment. The green line is the pointer originating from the manual controller. The light blue line represents the patient's skin. The model can be dragged around the room. The user can also zoom in and out. Background: MR workstation.

retinal display and was launched in August 2018. The device runs the Mixed Reality Viewer software that allows the creation of spatial-computing environments and the transport of images from the Elements Viewer software into the MR environment and the user's field of view (Figure 1). After wireless imaging transport from the Elements Viewer to the Mixed Reality Viewer, the user can inspect and interact with the object by using a manual controller. The user can rotate and drag the object as well as zoom in and out of the object. Up to four individual users wearing a Magic Leap One can observe and interact with the same object simultaneously. To allow adequate location of the object in the physical environment with multiple users, the users must visually scan a Mixed Reality Viewer positioning marker that serves as a reference point. Imaging transport from the Elements Viewer to the MR environment takes about 10–15 s. Further technical specifications and a video of the MRV in practice with the user's point of view are available in supplementary online materials.

Study population and imaging material

Preoperative CTAs of 50 patients with AAA were randomly selected from all patients who were treated electively with endovascular or open repair of infra- or juxtarenal AAA between 1 January 2018 and 31 December 2019 at the department of vascular and endovascular surgery. Arterial phase CTA series were used in all cases for the MRV and CV assessments. Axial, coronar, and sagittal reconstructions were provided for the CV assessment. All CTAs were anonymized before uploading it to the MR workstation. All CTA assessments were performed between 1 January 2021 and 1 March 2021 by two independent and experienced observers.

Standardized protocol

The protocol included four different item sets: calcification, dilatation, patency, and tortuosity. Furthermore, the number of visible lumbar and renal arteries was recorded. Detailed definitions and assessed vessel segments of the protocol are presented in Table 1. All assessments were timed using a conventional stopwatch.

Definitions

Calcification

Calcification was evaluated for 12 distinct vascular segments. The segments were: aorta (diaphragm to coeliac trunk), aorta (coeliac trunk to superior mesenteric artery), aorta (superior mesenteric artery to upper renal artery), aorta (infrarenal neck), common iliac arteries, internal iliac arteries, external iliac arteries, and common femoral arteries. Calcification of each segment was classified as "mild," "moderate," or "severe." Anterior and posterior aspects of the segments were classified separately. "Mild" was defined as an estimated ≤10% calcified surface area, "moderate" as > 10% and ≤50% calcified surface area, and "severe" was used when >50% of the surface area appeared calcified.[6]

Dilatation

Dilatation was evaluated in the same 12 segments as calcification. Each segment was classified as "normal," "ectatic," or "aneurysmatic." "Ectatic" was defined as an estimated diameter of >100% and ≤150% of the diameter of adjacent vessel segments. "Aneurysmatic" was used when the diameter was >150% of the adjacent diameters.[7]

Patency

Patency was evaluated in 13 different vascular segments. The segments were coeliac trunk, superior mesenteric artery, renal arteries, inferior mesenteric artery, common iliac arteries, internal iliac arteries, external iliac arteries, and common femoral arteries. Each of the 13 segments was classified as "low-grade stenosis" (including no stenosis), "high-grade stenosis," or "occlusion." High-grade stenosis was defined as ≥ 75% area stenosis without occlusion[8]

Iliac tortuosity

Iliac tortuosity was evaluated for the right and left iliac axis. The term "iliac axis" includes the common iliac and external iliac artery. Tortuosity was classified as "none," "mild," "moderate," or "severe." "None" was defined as no

Table 1. Assessed vessel segments and definitions of the standardized protocol.

Classification	Definition	Vessel segments
Calcification (anterior and posterior)		
Mild	≤10% calcified surface area	Aorta (diaphragm to CT); aorta (CT to SMA); aorta (SMA to upper RA); aorta (infrarenal neck); CIAs; IAs; EIAs; and CFAs
Moderate	>10 and ≤50% calcified surface area	
Severe	>50% calcified surface area	
Dilatation		
Normal	≤100% of adjacent vessel diameter	CT; SMA; RAs; IMA; CIAs; IIAs; EIAs; and CFAs
Ectatic	>100% and ≤150% of adjacent vessel diameter	
Aneurysmatic	>150% of adjacent vessel diameters	
Patency		
No or low-grade stenosis	<75% area stenosis	CT; SMA; RAs; IMA; CIAs; IIAs; EIAs; and CFAs
High-grade stenosis	≥75% area stenosis without occlusion	
Occlusion	Total luminal occlusion	
Tortuosity		
None	No angle ≥45°	Right iliac axis; left iliac axis
Mild	≥ One angulation >45° and ≤90°	
Moderate	one angulation ≥90°	
Severe	≥ Two angulations ≥90°	

CT: coeliac trunk; SMA: superior mesenteric artery; RA: renal artery; IMA: inferior mesenteric artery; CIA: common iliac artery; IIA: internal iliac artery; EIA: external iliac artery; CFA: common femoral artery.

angle ≥45°, "mild" was ≥ one angulation >45° and ≤90°, "moderate" was one angulation ≥90°, and "severe" was ≥ two angulations ≥90°.[9]

Statistical analysis

IA was calculated using Cohen's kappa (κ). Interpretation of resulting kappa values followed the originally proposed interpretation by Landis and Koch[10]. $\kappa < 0$ (poor agreement), 0 to 0.2 (slight agreement), 0.2 to 0.4 (fair agreement), 0.41 to 0.60 (moderate agreement), 0.61 to 0.80 (substantial agreement), and 0.81 to 1.0 ((almost) perfect agreement). The difference of the mean number of identified lumbar and renal arteries between the MRV and the CV was tested for statistical significance using the one sample t-test. Statistical significance was defined as $\alpha < 0.05$. Statistical analysis and production of figures were performed using R.[11]

Results

Patient population

Preoperative CTAs of 50 patients with AAAs were randomly selected from all patients who were treated electively with endovascular or open repair of infra- or juxtarenal AAA between 1 January 2018 and 31 December 2019 at the department of vascular and endovascular surgery. The median age was 72.9 (range: 52.7–85.3) years and five patients were female (10%).

Technical details

All 50 preoperative CTAs were successfully imported to the MR workstation and could subsequently be displayed in an MR environment using the Magic Leap One HMD (100%). Forty-two CTAs had a slice thickness of ≤1 mm. The remaining eight CTAs had a slice thickness of >1 and ≤3 mm.

Interobserver agreement (IA)

Calcification. IA of the MRV in the evaluation of calcification of the anterior as well as the posterior aspect of the aortoiliac vasculature was better when compared with the CV. The MRV demonstrated substantial agreement for the anterior ($\kappa = 0.68$, confidence interval (CI): 0.59–0.76) and posterior ($\kappa = 0.61$, CI: 0.53–0.69) calcification classification. With the CV, the IA in classifying the anterior and posterior surface areas of the aortoiliac vasculature was slight ($\kappa = 0.33$, CI: 0.14–0.51) and fair ($\kappa = 0.45$, CI: 0.35–0.56), respectively. When using the MRV, both observers

classified calcification as more severe. Observer 1 and observer 2 classified 100/588 (17.0%) and 96/588 (16.3%) anterior and 129/586 (22.0%) and 125/586 (21.3%) posterior segments as moderately or severely calcified. Correspondingly for the CV, observer 1 and observer 2 classified 34/574 (5.9%) and 40/574 (7.0%) anterior and 75/577 (13.0%) and 103/577 (17.9%) posterior segments as moderately or severely calcified.

Dilatation

The MRV and the CV each demonstrated substantial IA in the assessment of dilatations in the aortoiliac vasculature. (κ = 0.68, CI: 0.59–0.78 and κ = 0.67, CI: 0.58–0.77, respectively) Using the CV, the two observers agreed in the classification of 547/588 segments (93.0%). When using the MRV, the two observers agreed in 550/590 segments (93.2%). In the CV as well as in the MRV assessment, disagreement was present almost exclusively in the differentiation of adjacent classes. In the CV, all 41 segments with disagreement were either classified ectatic by observer 1 and normal by observer two or aneurysmatic by observer 1 and ectatic by observer 2 and vice versa. There were no cases of aneurysmatic classification by one observer and normal classification by the other observer in the CV. In the MRV, there was one segment that was classified aneurysmatic by one observer and normal by the other observer (0.2%). The remaining 39 segments with disagreement were misclassified into the adjacent classes.

Patency

IA of the CV in the assessment of vessel patency was almost perfect (κ = 0.93, CI: 0.86–1.00). The MRV performed worse but still demonstrated substantial agreement between observers (κ = 0.74, CI: 0.61–0.86). When using the CV, the two observers disagreed in the classification of 4 segments (0.6%). Correspondingly, when using the MRV, the two observers disagreed in the classification of 17 segments (2.7%). In 6/17 cases, the two observers did not agree, if a vessel segment was occluded or patent.

Tortuosity

The MRV and the CV both showed fair agreement between observers in the assessment of iliac tortuosity. The MRV demonstrated slightly better agreement (κ = 0.60, CI: 0.47–0.73) compared with the CV (κ = 0.48, CI: 0.34–0.62). When using the CV, the two observers agreed in 65/100 (65.0%) assessments of iliac tortuosity. Disagreement was present in the differentiation of adjacent classes in 30/35 cases (85.7%). Correspondingly, when using the MRV, the two observers agreed in 72/100 (72%) assessments. Disagreement was present in 26/28 cases (92.9%) in the differentiation of adjacent classes. Results of assessments of calcification, dilatation, patency, and tortuosity assessments are summarized in contingency Table 2, Table 3, and Figure 2.

Number of lumbar arteries

The two observers identified a mean of 3.8 (standard deviation (SD): 2.1) lumbar arteries (LA) in the CV and 2.4 (SD: 1.9) LAs in the MRV, which collectively adds up to a total of 379 identified LAs in the CV and 239 LAs in the MRV in all 50 patients ($p < 0.01$, one sample t-test).

Number of renal arteries

Overall, the two observers identified a mean of 2.3 (SD 0.8) and 2.4 (SD 0.8) renal arteries (RA) ($p = 0.16$). In total, there were 231 RAs identified in the CV and 236 RAs in the MRV. Identification of LAs and RAs is summarized in Table 4 and Figure 3.

Duration of the assessment

The mean duration of assessment in the CV was 4.6 min (SD 1.6), and in the MRV, it was 4.0 min (SD 1.7). ($p < 0.01$, one sample t-test).

Discussion

This is the first study investigating the feasibility of a MR viewer (MRV) application designed to produce high-quality holograms of aortoiliac anatomy of AAA patients for routine clinical use. The interobserver agreement (IA) of the assessment of aortoiliac anatomy in the MR environment was calculated as a measure of reliability and compared with the IA when using multi-planar reconstructions of arterial phase CTA in a conventional viewer software application. IA was calculated for four sets of items: calcification, dilatation, tortuosity, and patency.

IA when using the MRV was superior in the assessment of calcification when compared with the CV. The three-dimensional holographic visualization allowed a more intuitive understanding of the overall calcification load as well as the orientation of calcification on the anterior and posterior aspects of the vessel segments compared to the fractioned view of planar reconstructions. Interestingly, when confronted with the three-dimensional reconstruction, both observers classified calcification as being more severe than in the CV. It must be noted, however, that IA is a measure of reliability and does not allow conclusions with regards to the validity of the estimate. CTA in general tends to overestimate calcification load and since the MR reconstruction is merely a derivative of CTA, the MRV is expected to equally overestimate calcification.[12]

Table 2. Interobserver agreement in the assessment of calcification, dilatation, patency, and tortuosity.

	CV					—	MRV				
Calcification anterior											
κ	0.33 (0.14–0.51)					κ	0.68 (0.59–0.76)				
N	574					***N***	588				
Observer 2	Observer 1					Observer 2	Observer 1				
	—	1	2	3			—	1	2	3	
	1	517	16	1			1	470	22	0	
	2	22	9	6			2	18	47	5	
	3	1	1	1			3	0	10	16	
Calcification posterior											
κ	0.45 (0.35–0.56)					—	0.61 (0.53–0.69)				
N	577					—	586				
Observer 2	Observer 1					—	Observer 1				
	—	1	2	3		Observer 2	—	1	2	3	
	1	455	18	1			1	430	29	2	
	2	44	30	8			2	25	57	8	
	3	3	11	7			3	2	16	17	
Dilatation											
κ	0.67 (0.58–0.77)					—	0.68 (0.59–0.78)				
N	588					—	590				
—	Observer 1					—	Observer 1				
Observer 2	—	1	2	3		Observer 2	—	1	2	3	
	1	504	19	0			1	504	20	1	
	2	12	17	1			2	12	25	4	
	3	0	9	26			3	0	3	21	
Patency											
κ	0.92 (0.86–1.00)					—	0.74 (0.61–0.86)				
N	628					—	629				
—	Observer 1					—	Observer 1				
Observer 2	—	1	2	3		Observer 2	—	1	2	3	
	1	597	0	2			1	587	8	2	
	2	2	10	0			2	3	9	0	
	3	0	0	17			3	4	0	16	
Tortuosity											
κ	0.48 (0.34–0.62)					—	0.6 (0.47–0.73)				
N	100					—	100				
—	Observer 1					—	Observer 1				
Observer 2	—	1	2	3	4	Observer 2	—	1	2	3	4
	1	5	3	1	0		1	10	5	0	0
	2	6	30	8	1		2	3	27	5	2
	3	3	4	25	7		3	0	3	28	2
	4	0	0	2	5		4	0	0	8	7

Cohen´s kappa κ (95% confidence interval); CV: conventional viewer; MRV: mixed Reality viewer; the gray diagonal in the contingency tables represents cases of perfect agreement between both observers. Classifications are displayed as numerical.

Additionally, since the automatic MRV vascular reconstruction can only be based on arterial or venous phase CTA, no native phase CT can be displayed for calcification assessment in a three-dimensional reconstruction. Nonetheless, extensive CT-morphological vessel calcification is associated with an increased risk for access-related complications during endovascular interventions and accurate assessment of calcification constitutes an important consideration for open vascular surgery as well.[13-15]

Aortoiliac dilatation was assessed with substantial IA in both modalities. One major drawback of the current version of the MRV is that there is no option to perform quantitative diameter measurements in the MR environment yet. In the present study, no quantitative measurements of diameter were performed in the CV either, which results in a similar interobserver agreement. However, by this deficiency alone, the MRV in its current version cannot be used for more advanced planning purposes like

EVAR device selection and sizing or even decision making regarding surgical indication or follow-up evaluation. Future updates of the MRV will include the option to perform basic diameter measurements in the MR environment. To use the MR viewer as EVAR planning tool, however, would furthermore require centerline reconstructions which are currently not available.

Iliac tortuosity is associated with increased risk for complications following EVAR like stent graft limb occlusion and endoleak.[16] Additionally, it can limit technical applicability of EVAR.[17-19] Despite its importance, objective assessment of iliac tortuosity is challenging in clinical routine. Therefore, tortuosity is often evaluated based on subjective assessment. In the present study, subjective tortuosity assessment using the MRV demonstrated a trend toward higher IA when compared to the CV. As expected, three-dimensional and complex structures like iliac angulations and curvatures can be understood more naturally as an object in a three-dimensional environment than in multi-planar reconstructions.

While the MRV demonstrated its strength in the visualization of vascular anatomic characteristics that are especially depending on three dimensions like calcification and tortuosity, limitations in visualization of more delicate structures like lumbar arteries and stenosis became also apparent. While there was no statistically significant difference in the number of detected renal arteries, the two observers detected significantly less lumbar arteries, which usually have smaller diameters. Additionally, the CV demonstrated higher IA in the assessment of vessel patency which is also dependent on higher resolution images. The reason for this loss of information on the side of the MRV when dealing with smaller structures is to be found in the

Table 3. Interobserver agreement of two observers using either the conventional viewer or the Mixed Reality Viewer.

	Conventional viewer		Mixed Reality Viewer	
	κ	95% CI	κ	95% CI
Calcification anterior	0.33	0.14–0.51	0.68	0.59–0.76
Calcification posterior	0.45	0.35–0.56	0.61	0.53–0.69
Dilatation	0.67	0.58–0.77	0.68	0.59–0.78
Patency	0.93	0.86–1.00	0.74	0.61–0.86
Tortuosity	0.48	0.34–0.62	0.60	0.47–0.73

Cohen´s kappa κ

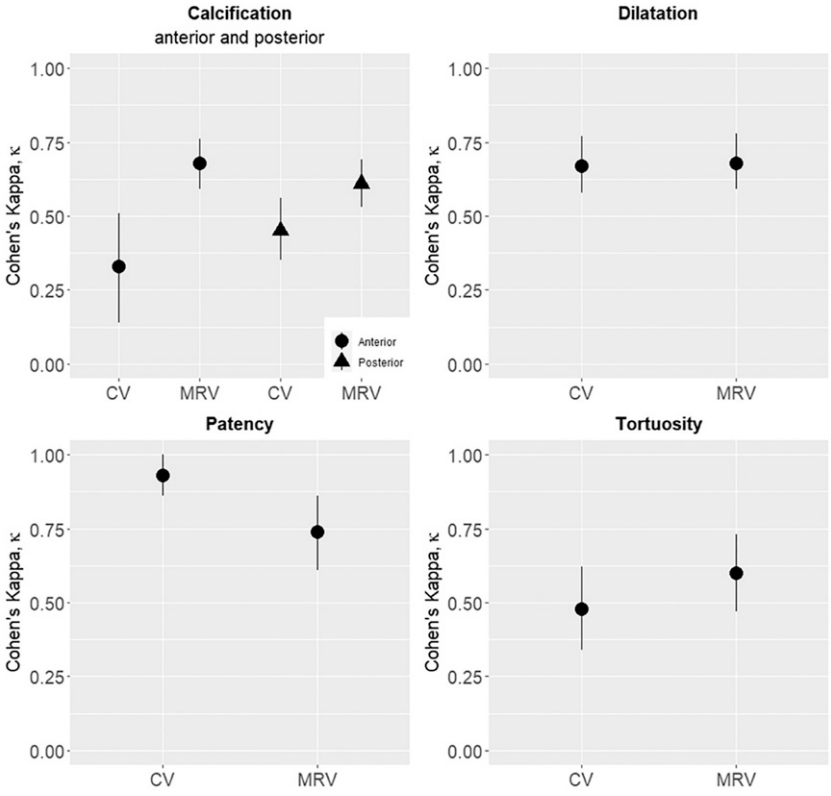

Figure 2. Interobserver agreement expressed as Cohen´s kappa (κ) in the assessment of calcification, dilatation, patency, and tortuosity. Cohen´s kappa (κ) is represented by a dot or triangle, respectively. The 95% confidence interval is represented by a vertical line. CV: conventional viewer, MRV: Mixed Reality Viewer. Numerical values of Cohen´s kappa κ are represented in Table 3.

Table 4. Mean and absolute numbers of lumbar and renal arteries.

	Conventional viewer		Mixed Reality Viewer		
	Mean (SD)	Total	Mean (SD)	Total	*p* value*
Lumbar arteries	3.8 (2.1)	379	2.4 (1.9)	239	<0.01
Renal arteries	2.3 (0.8)	231	2.4 (0.8)	236	0.16

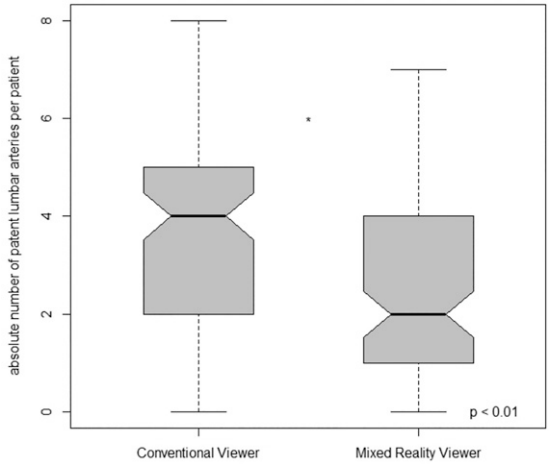

Figure 3. Absolute number of lumbar arteries per patient in the conventional viewer and in the Mixed Reality Viewer. One sample t-test. Numerical values of the absolute number of patent lumbar arteries are represented in Table 4.

process of three-dimensional reconstruction and display of that reconstruction in the MR environment. The quality of the reconstruction and subsequently the hologram is a function of the method used for reconstruction, quality of underlying CTAs, slice thickness, and contrast volumes, as well as hardware specifications that are required to continuously update the three-dimensional hologram in the MR environment when the observers move around the object in real time. Overall, deficiencies in visualization of smaller structures are currently mainly limited by technical specifications and improvements are to be expected in the future.

There are several limitations of this study to consider. This study examined interobserver agreement as a measure of reliability. It did not however examine the validity of the assessment as this would require the measurement of actual physical vessel calcification or patency in which cases a gold standard is difficult to obtain as a reference. Additionally, this study only analyzed MR using a specific set of hard- and software and was focused on aortoiliac vascular anatomy only and conclusions might not apply to a different technical setup and to other areas of interest. Furthermore, this study compared CTA assessments in multi-planar reconstructions as it is clinical practice in daily routine and compared results with three-dimensional reconstructions using the isosurface-volume-rendering method in a MR environment. Observed differences in IA might as well be expected when using conventional three-dimensional reconstructions on a two-dimensional monitor and can therefore not exclusively be attributed to the MR application. However, compared to conventional three-dimensional reconstruction, the MR hologram has the potential to be registered to the physical patient in the future and thereby facilitate navigation in open and endovascular surgery as well as vascular access. MR technology has the potential to improve navigational accuracy and to reduce radiation for patients and surgeons alike. While clearly these MR-based technologies are still at the very beginning and further research and development is necessary before this potential can be translated into clinical reality, the registration of holograms with physical objects in a medical context has already been investigated in some pilot studies and demonstrated promising initial results.[20-22] Additionally, three-dimensional holograms in a MR environment can be used in medical education, simulation training, or in patient education during informed consent.[23-26] Another limitation is that this is a single center exploratory pilot study demonstrating feasibility of a new CTA visualization technology which needs to be investigated in future studies before final conclusions with regards to its true future clinical use can be made.

In summary, this study demonstrated that the MRV can be used as a complementary imaging viewing technology that allows the production of holograms based on routine CTA data. Additionally, the holographic display had its strength in the visualization of structures that are especially depending on three-dimensional orientation. Nonetheless, it was also demonstrated that there are deficiencies in the display of smaller structures like vessel stenosis, which is highly relevant for practical clinical applications.

However, to truly exploit the full potential of MR technology in endovascular or open surgery, it is paramount to not only investigate accurate registration of the hologram with the physical patient as some studies already have, but to also advance efforts aimed at measuring and improving the quality of underlying holograms like in the present study.[4, 27] Applications that allow pragmatic production of high-quality holograms are a prerequisite for wide-spread MR technology adoption in the future. By registering a high-resolution virtual image with the physical patient and thereby establishing both components as obligatory elements of a clinical application, the MRV will prove to be a useful and inevitable tool in the hands of clinicians.

Conclusion

The MRV is a feasible imaging viewing technology in clinical routine and showed improved interobserver agreement (IA) in the assessment of items that are especially

depending on three-dimensional orientation. There are deficiencies in the visualization of smaller vessels and vessel patency, which is of high relevance for MR applications in vascular medicine. Future efforts should aim at improving hologram quality and enabling accurate registration of the hologram with the physical patient.

Declaration of conflicting interests

The author(s) declared no potential conflicts of interest with respect to the research, authorship, and/or publication of this article.

Funding

The author(s) received no financial support for the research, authorship, and/or publication of this article.

Ethical approval

Ethical approval was obtained by the local ethics committee. (S727/2020)

Informed consent

Was waved according to ethical approval (S-727/2020)

ORCID iD

Johannes Hatzl https://orcid.org/0000-0002-3152-7791

References

1. Hu H-Z, Feng X-B, Shao Z-W, et al. Application and prospect of mixed reality technology in medical field. *Curr Med Sci* 2019; 39: 1–6. DOI: 10.1007/s11596-019-1992-8
2. Rynio P, Witowski J, Kamiński J, et al. Holographically-guided endovascular aneurysm repair. *J Endovascular Ther* 2019; 26: 544–547. DOI: 10.1177/1526602819854468
3. Böckler D, Geisbüsch P, Hatzl J, et al. Erste Anwendungsoptionen von künstlicher Intelligenz und digitalen Systemen im gefäßchirurgischen Hybridoperationssaal der nahen Zukunft. *Gefässchirurgie* 2020; 25: 317–323. DOI: 10.1007/s00772-020-00666-9
4. García-Vázquez V, von Haxthausen F, Jäckle S, et al. Navigation and visualisation with HoloLens in endovascular aortic repair. *Innovative Surg Sci* 2018; 3: 167–177. DOI: 10.1515/iss-2018-2001
5. Viera AJ and Garrett JM. Understanding interobserver agreement: the kappa statistic. *Fam Medicine* 2005; 37: 360–363. DOI: 2005/05/11
6. Mousa AY, Campbell JE, Broce M, et al. Predictors of percutaneous access failure requiring open femoral surgical conversion during endovascular aortic aneurysm repair. *J Vasc Surg* 2013; 58: 1213–1219. DOI: 10.1016/j.jvs.2013.04.065
7. Johnston KW, Rutherford RB, Tilson MD, et al. Suggested standards for reporting on arterial aneurysms. *J Vasc Surg* 1991; 13: 452–458. DOI: 10.1067/mva.1991.26737
8. Diehm N, Pattynama PM, Jaff MR, et al. Clinical endpoints in peripheral endovascular revascularization trials: a case for standardized definitions. *Eur J Vasc Endovascular Surg* 2008; 36: 409–419. DOI: 10.1016/j.ejvs.2008.06.020
9. Kristmundsson T, Sonesson B and Resch T. A novel method to estimate iliac tortuosity in evaluating EVAR access. *J Endovascular Ther* 2012; 19: 157–164. DOI: 10.1583/11-3704.1
10. Landis JR and Koch GG. The measurement of observer agreement for categorical data. *Biometrics* 1977; 33: 159–174. DOI: 1977/03/01.
11. R Core Team. R. *A Language and Environment for Statistical Computing*. Vienna, Austria: R Foundation for Statistical Computing, 2019.
12. Buijs RVC, Leemans EL, Greuter M, et al. Quantification of abdominal aortic calcification: Inherent measurement errors in current computed tomography imaging. *PLoS One* 2018; 13: e0193419. DOI: 10.1371/journal.pone.0193419
13. Babin-Ebell J, Gimpel-Henning K, Sievers H-H, et al. Influence of clamp duration and pressure on endothelial damage in aortic cross-clamping. *Interactive CardioVascular Thorac Surg* 2010; 10: 168–171. DOI: 10.1510/icvts.2009.220996
14. Schneider J., Gottner RJ and Golan JF. Supraceliac versus infrarenal aortic cross-clamp for repair of non-ruptured infrarenal and juxtarenal abdominal aortic aneurysm. *Cardiovasc Surg* 1997; 5: 279–285. DOI: 10.1016/s0967-2109(97)00021-5
15. Manunga JM, Gloviczki P, Oderich GS, et al. Femoral artery calcification as a determinant of success for percutaneous access for endovascular abdominal aortic aneurysm repair. *J Vasc Surg* 2013; 58: 1208–1212. DOI: 10.1016/j.jvs.2013.05.028
16. Wolf YG, Tillich M, Lee WA, et al. Impact of aortoiliac tortuosity on endovascular repair of abdominal aortic aneurysms: evaluation of 3D computer-based assessment. *J Vasc Surg* 2001; 34: 594–599. DOI: 10.1067/mva.2001.118586
17. Tillich M, Bell RE, Paik DS, et al. Iliac arterial injuries after endovascular repair of abdominal aortic aneurysms: correlation with iliac curvature and diameter. *Radiology* 2001; 219: 129–136. DOI: 10.1148/radiology.219.1.r01ap15129
18. Wolf YG, Fogarty TJ, Olcott C, et al. Endovascular repair of abdominal aortic aneurysms: eligibility rate and impact on the rate of open repair. *J Vasc Surg* 2000; 32: 519–523. DOI: 10.1067/mva.2000.107995
19. Coulston J, Baigent A, Selvachandran H, et al. The impact of endovascular aneurysm repair on aortoiliac tortuosity and its use as a predictor of iliac limb complications. *J Vasc Surg* 2014; 60: 585–589. DOI: 10.1016/j.jvs.2014.03.279
20. Groves L, Li N, Peters TM, et al. Towards a first-person perspective mixed reality guidance system for needle interventions. *J Imaging* 2022; 8: 7–21. DOI: 10.3390/jimaging8010007
21. Wesselius TS, Meulstee JW, Luijten G, et al. Holographic augmented reality for DIEP flap harvest. *Plast Reconstr Surg* 2021; 147: 25e–29e. DOI: 10.1097/prs.0000000000007457

22. Teatini A, Kumar RP, Elle OJ, et al. Mixed reality as a novel tool for diagnostic and surgical navigation in orthopaedics. *Int J Comp Assist Radiol Surg* 2021; 16: 407–414. DOI: 10.1007/s11548-020-02302-z
23. Schoeb DS, Schwarz J, Hein S, et al. Mixed reality for teaching catheter placement to medical students: a randomized single-blinded, prospective trial. *BMC Medical Education* 2020; 20: 510. DOI: 510. 2020/12/1810.1186/s12909-020-02450-5
24. House PM, Pelzl S, Furrer S, et al. Use of the mixed reality tool "VSI Patient Education" for more comprehensible and imaginable patient educations before epilepsy surgery and stereotactic implantation of DBS or stereo-EEG electrodes. *Epilepsy Res* 2020; 159: 106247. DOI: 10.1016/j.eplepsyres.2019.106247
25. Ruthberg JS, Tingle G, Tan L, et al. Mixed reality as a time-efficient alternative to cadaveric dissection. *Med Teach* 2020; 42: 896–901. DOI: 10.1080/0142159x.2020.1762032
26. Kovoor JG, Gupta AK and Gladman MA. Validity and effectiveness of augmented reality in surgical education: a systematic review. *Surgery* 2021; 170: 88–98. DOI: 10.1016/j.surg.2021.01.051
27. Mitsuno D, Ueda K, Hirota Y, et al. Effective application of mixed reality device hololens. *Plast Reconstr Surg* 2019; 143: 647–651. DOI: 10.1097/prs.0000000000005215